IEEE Access
Multidisciplinary | Rapid Review | Open Access Journal

Received 10 March 2024, accepted 26 March 2024, date of publication 29 March 2024, date of current version 9 April 2024.

Digital Object Identifier 10.1109/ACCESS.2024.3383139

RESEARCH ARTICLE

Performance Analysis of Joint Radar-Communication System Based on FDA-MIMO Radar

MENGJIAO LI AND WEN-QIN WANG, (Senior Member, IEEE)
School of Information and Communication Engineering, University of Electronic Science and Technology of China, Chengdu 610000, China
Corresponding author: Wen-Qin Wang (wqwang@uestc.edu.cn)

ABSTRACT Faced with the increasingly complicated electromagnetic environment, the joint design of radar and communication system has been an effective solution to save spectrum resources and reduce the complexity of system hardware. By introducing index modulation, we design a joint radar-communication system based on the frequency diverse array (FDA) based multiple-input-multiple-output (MIMO) radar. Different from the conventional phased-array (PA) radar and MIMO radar array, the FDA-MIMO radar can generate range-angle-dependent beampattern, which enables the distinctive signal processing methods. In this paper, we proceed the investigation on performance analysis of the proposed joint system scheme by firstly establishing the three-dimension (3D) signal model for the radar subsystem, based on which the achievable radar resolution in range, angle and Doppler dimension can be estimated. Since the beampattern of FDA-MIMO radar is range-dependent, the joint system can achieve interference suppression against the false targets in radar mainlobe. For communication subsystem, a communication security enhancement approach is proposed, followed by the derivation of theoretical symbol error rate (SER) upper bound. The numerical results demonstrate the effectiveness and superiority compared with the other dual-function systems based on conventional multi-antenna arrays.

INDEX TERMS FDA-MIMO radar, joint radar-communication system, range-angle-dependent beampattern, radar resolution, interference suppression, communication security enhancement.

I. INTRODUCTION

The joint radar and communication system design has received extensive attention and in-depth research for its advantage on saving spectrum resources and reducing the complexity of system hardware. Concurrently, the main implementation methods for the integrating of radar and communication functionalities include coexistence approach, waveform design, and dual-functional system design. The coexistence approach consist in designing a unified framework, by sharing the beam or spectrum of radar and communication systems [1], [2], [3], [4], [5], [6], [7]. In [1] and [3], multiple beams towards radar targets and communication receivers at different directions are generated by optimizing the beampattern with specific rules. The spectrum sharing lies in that the collocated MIMO radar and MIMO communication locate on a single platform but operate separately, one system worked as the primary function while the other one worked as the interference [2], [4], [5], [6]. The waveform design approach aims to devise a dual-function signal model which can simultaneously deal with radar detection and information transmission [8], [9], [10], [11], by virtue of devising a dual functional signal [12], directly utilizing the communication signal [8] or waveform optimization based on MIMO radar [9], [10], [11]. The dual-function system design is to fuse communication functionality in the existing radar platform without perceptible impact on radar performance [13], [14], [15], [16], [17], [18]. For instance, the information bits can be embedded into radar pulses [13], sidelobe levels [14] and phases [15]. However, the communication data rate is rather low due to the limited degrees of freedom (DOFs).

Index modulation (IM) techniques, which utilize the indices of the active transmit antennas to convey additional

The associate editor coordinating the review of this manuscript and approving it for publication was Mohamed M. A. Moustafa.

information bits, are proposed as a digital modulation scheme for massive MIMO system due to its high spectral and energy efficiency [19], [20]. In recent years, it has attracted great interests as a new type of information embedding scheme in system design of dual-functional radar and communication (DFRC) system [7], [16], [17], [21], [22], [23], [24]. To differentiate from the frequency index modulation, it can be termed as spatial index modulation [16]. The frequency index modulation refers to embed information by the shuffling of the waveform with different frequencies [21], [22]. The spatial index modulation and frequency index modulation are both regarded as index modulation. In [25], two information embedding strategies based on IM are proposed for the MIMO DFRC system, that is, antenna-selection and hybrid selection and permutation. Based on the traditional phase array (PA) radar, the spatial modulation based communication radar (SpaCoR) system proposed are designed to embed information by combining communication modulation and spatial IM [23]. The multi-carrier agile joint radar and communication (MAJoRCom) system utilize the spatial and frequency index modulation to convey messages [16], [26]. Based on spatial index modulation, an antenna-selection-based transmit beamformer design strategy is proposed by maximizing the minimum target power in target directions [7].

At present, most researches on the design of radar and communication dual-function system based on a multi-antenna system mainly focus on PA and MIMO radar, which provides only angle-dependent transmit beampattern. The frequency diverse array (FDA) can generate a range-angle-time-dependent transmit beampattern due to the employment of a small frequency increment across the adjacent array elements [27], [28], [29]. The range-dependent transmit beampattern has become an increasingly important requirement in many applications, such as range-dependent interference and clutter suppression, directional communications and range ambiguity suppression [30], [31]. Due to the frequency offset, FDA radar can easily achieve orthogonal transmission by using a sufficiently large frequency offset or a orthogonal waveform set, that is FDA-MIMO radar [32], [33]. We call FDA radar, FDA-MIMO radar and some related designed array as FDA-based radar array, they both can offer extra DOFs in the range domain. The range and angle are coupled in the transmit beampattern for FDA-based radar, resulting in an S-shaped energy distribution in the range-angle plane, making them can fulfill some practical tasks that the conventional PA or MIMO radar cannot accomplish.

Some attempts have been made to design an integrated radar and communication systems based on FDA-based radar array [18], [34], [35], [36]. In [34], a dual-function FDA-MIMO system is designed by utilizing Costas frequency waveforms modulated with phase shift keying (PSK) modulation. An adaptive selection of high gain mainlobe and sidelobe controls the beam-pattern generated by frequency diversity array (FDA) based on the changes in joint radar and communication tracking applications are proposed in [36]. A Physical-Layer security technique for FDA Communications are discussed in [35]. Besides, in our proposed joint radar-communication system based on FDA-MIMO radar [37], the combination of frequency index modulation and phase modulation can achieve data transmission as well as synthesizing a range-angle dependent beampattern.

Based on these discussions, it is anticipated that the proposed joint radar-communication system based on FDA-MIMO radar, which simultaneously utilize IM and phase modulation to embed information bits, can provides some distinct performance compared with the dual-function systems based on the traditional PA and MIMO radar arrays. The randomization in frequency offsets not only inherently coincide with index modulation, but also decouples the range and angle at the same time. The range-angle-dependent beampattern also brings new opportunities and challenges. Hence, in this paper, we proceed to investigate the performance of the joint radar-communication system based on FDA-MIMO radar. The main contributions are listed as follows:

1) The range-angle-Doppler 3D signal model is built, based on which the range-space-time (RST) response is introduced to estimate the radar resolution in range, angle and Doppler profile.
2) Since FDA-MIMO radar can generate range-angle dependent beampattern, the radar subsystem of the proposed joint system can suppress the interference caused by jammers with different ranges and angles. An eigenvalue projection and blocking matrix processing are employed as the mainlobe interference suppression algorithm instead of the conventional MVDR method.
3) Inspired by the directional modulation [38], [39], of which the principle is to modulate the phase of the transmit signals on different antennas of PA radar, we put forward an communication security enhancement approach by maximizing the signal power in the desired direction of the target user.
4) The upper bound of the SER is theoretically deduced, which can help to determine communication modulation mode for trading off data rate and system reliability.

The remainder of this paper is organized as follows. Section II presents the system and signal model of the proposed joint system, including the information embedded approach, the three-dimension signal model for the radar subsystem and the information demodulation process for the communication subsystem. In Section III, the radar resolution in range, angle and Doppler are provided. Section IV formulates the mainlobe interference suppression methods. The communication security enhancement approach and the derivation of SER upper bound are given in Section V and Section VI, respectively. The simulation results and the performance analysis of the proposed joint system are presented in Section VII. Finally, conclusions are drawn in Section VIII.

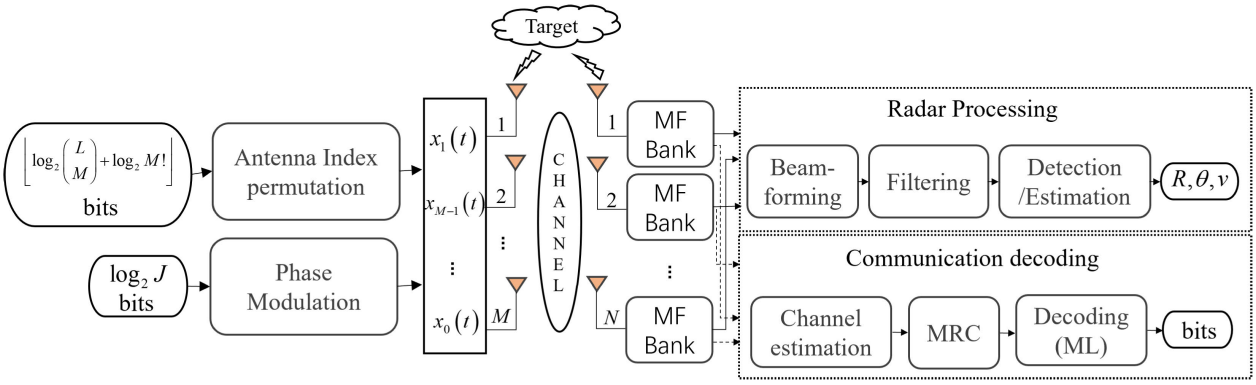

FIGURE 1. Joint radar and communication system model with M transmit and N receive antennas.

II. SYSTEM AND SIGNAL MODEL

In this section we review the proposed joint radar and communication system model based on FDA-MIMO radar. We first present the information embedding approach and how this model differentiate from the other dual-function systems that are designed based on PA and MIMO radar in Section II-A. Then, the received signal model and signal processing of radar subsystem and communication subsystem are elaborated in Section II-B and Section II-C, respectively.

A. THE JOINT SYSTEM MODEL

The transmit and receive system diagram of the joint radar and communication system based on FDA-MIMO is illustrated in Fig.1. The multiple-antenna arrays is composed of M transmit elements and N receive elements which are both equally spaced by d. Functionally, the joint system can be divided into radar subsystem and communication subsystem. The radar subsystem can apply the normal radar signal processing flow, including waveform beamforming, matched filtering and parameter detection. For communication subsystem, the maximum ratio combining (MRC) technique to improve the accuracy of the decoding by taking advantage of waveform diversity, followed by the communication decoding with maximum likelihood (ML). Notablely, the traditional receiving methods is not suitable for FDA-based radar system, because the range-related phase may be cancelled for the sake of the time-variance of FDA-MIMO transmit beampattern, as demonstrated in [31]. Thus, we adopt the multi-channel receiver structure for the proposed joint system based on FDA-MIMO radar [37]. The receiver utilizes a group of matched filter bank to demodulate the echo signals, as shown in Fig.2, each matched filter bank consists of multiple mixers and different multiple matched filters, so that the range-dependent transmit beampattern can be retained, which is undoubtedly the main feature that distinguishes FDA radar from the traditional PA and MIMO radar arrays.

In the proposed joint radar and communication system based on FDA-MIMO radar, the information embedding approach adopts the classic phase modulation (PM) and index modulation via permutation (IMP). The index modulation exploit the inherent randomness in the selection of carrier frequencies and their allocation among the transmit antennas to convey information. The phase modulation is inserting an equivalent phase term in all the transmit signals of each radar pulse. We can notice that the design principle of the overall information embedding scheme lies in that it basically have no or minimal impact on radar functionality.

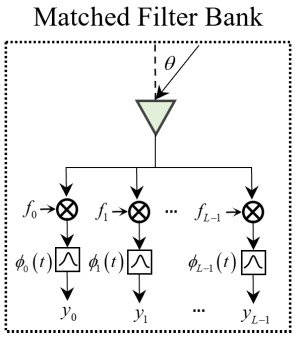

FIGURE 2. Matched filter bank in a single antenna.

To demonstrate the rationality and feasibility, we make a comparison of the transmit-receive beampattern of MIMO, linear FDA-MIMO (LFDA-MIMO), the proposed random FDA-MIMO (RFDA-MIMO) based on waveform permutations, and the antenna-selected-based RFDA-MIMO, the results are shown in Fig.3. The transmit-receive beampattern of conventional MIMO and FDA-MIMO radar are depicted in Fig.3(a) and Fig.3(b), it's clear that the difference of two systems lies in that the beampattern of MIMO radar is only angle-dependent, while the FDA-MIMO radar can have range-dependent in the transmit-receive beampattern. Compared with Fig.3(c), the beampattern of antenna-selected RFDA-MIMO in Fig.3(d) is no longer ideal thumbtack-like in range-angle plane, resulting in serious range ambiguities. For this reason, we merely consider the index modulation via waveform permutation to be applied

in the proposed joint radar and communication system design.

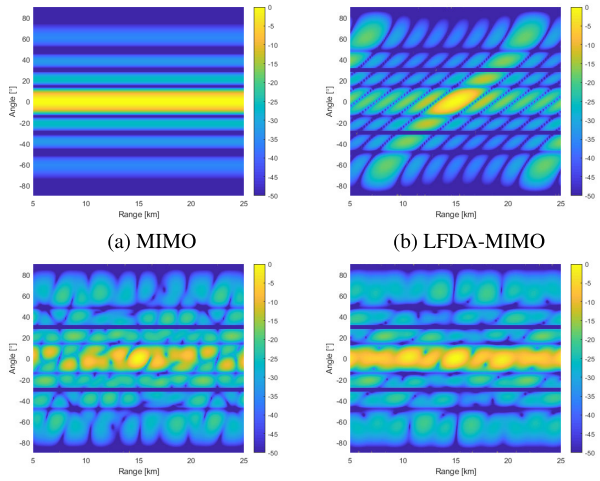

(a) MIMO (b) LFDA-MIMO

(c) RFDA-MIMO (d) Antenna-selected RFDA-MIMO

FIGURE 3. The transmit-receive beampattern of different antenna arrays.

For the conventional FDA-MIMO radar, the transmit signals are orthogonal with linear frequency increments along the array elements. The transmit signal on the mth element of FDA-MIMO radar can be represented as

$$s_m(t) = \phi_m(t) e^{j2\pi(f_c+(m-1)\Delta f)t} \tag{1}$$

where f_c is the reference carrier frequency and Δf is the frequency offset of different signals. $\phi_m(t)$ denotes the complex envelope of baseband waveform with unit energy, and satisfies the orthogonal and frequency shift orthogonal condition, which is

$$\begin{aligned} \int_T \phi_m(t)\phi_m^*(t)dt &= 1 \\ \int_T \phi_m(t)\phi_n^*(t)dt &= 0, m \neq n \\ \int_T \phi_m(t)\phi_n^*(t-\tau)e^{j2\pi\Delta f(m-n)t}dt &= 0, \ \forall\tau, m \neq n \end{aligned} \tag{2}$$

where T is radar pulse duration and the superscript $*$ stands for the conjugate operator. Suppose there are K transmit pulses during the coherent processing interval (CPI). Then, in the kth radar pulse, the proposed random FDA-MIMO signal transmitted on the mth element is given by

$$x_{k,m}(t) = \sqrt{\frac{E}{M}}\phi_m(t - kT_{PRI}) e^{j2\pi f_{p_m}t} e^{j\varphi_k} \tag{3}$$

where E is the total transmit energy and T_{PRI} denotes the pulse repetition interval (PRI). The carriers frequencies $f_{p_m} = f_c + p_m\Delta f$ is not linearly distribution, it is chosen from the frequency set $\mathcal{F} = \{f_m = f_c + m\Delta f \,|m \in \mathcal{M}\}$, $\mathcal{M} = \{0, 1, \ldots, M-1\}$. The phase term $e^{j\varphi_k}$ is used to embed additional information in kth pulse through phase modulation, which are chosen from a predefined constellation. Herein, we consider the constellation is distributed uniformly in $[0, 2\pi]$, that is, $\mathcal{Q} = \left\{0, \frac{2\pi}{J}, \ldots, \frac{2\pi(J-1)}{J}\right\}$. $\varphi_k \in \mathcal{Q}, k = \{0, 1, \ldots, K-1\}$.

The information bits are embedded by combining PM and IMP methods in the proposed joint radar and communication system, the whole process can be divided into three steps. First, there are $L, L > M$ available orthogonal waveform with different frequency offset, the baseband waveform set is denoted by $\mathcal{S} = \{s_l(t)\}_{l=0}^{L-1}$, where $s_l(t) = \phi_l(t) e^{j2\pi l\Delta ft}$. $\binom{L}{M}$ possible combinations of carrier frequencies that can be selected, where $\binom{\cdot}{\cdot}$ denotes the Binomial coefficient. Next, the selected waveform are randomly assigned to the selected transmit antennas, there are $M!$ possible permutations. After these two steps, the index and permutation modulation is completed, and the information bits it can convey is $\lfloor \log_2\binom{L}{M} + \log_2 M! \rfloor$, where $\lfloor\cdot\rfloor$ is the floor function. Finally, the phase modulation is utilized to improve the data rate, which can be easily realized with a phase shifter. Suppose there are totally J phase values, the number of bits it can convey through the phase modulation in the final steps should be $\log_2 J$. Hence, the total number of information bits it can convey in each pulse is $\log_2 J + \left\lfloor \log_2\binom{L}{M} + \log_2 M! \right\rfloor$. The total bit rate of the proposed system scheme in each CPI should be

$$R_b = K \cdot \left(\log_2 J + \left\lfloor \log_2\binom{L}{M} + \log_2 M! \right\rfloor\right) \cdot f_{PRF} \tag{4}$$

B. RADAR SUBSYSTEM

Without loss of generality, the transmit antennas of the joint system are considered to be colocated in the default target detection scenarios, such that a target in the far-field would be seen from the same direction angle. Suppose the synthesized signals of the M transmit antennas are emitted and arrive at a given far-field point target (r, θ, v), and then be reflected to the multiple-antenna receiver. We define $\Theta = (r, \theta, v)$, the returned signal from the mth transmit element to the nth receive element of the kth pulse can be expressed as

$$\begin{aligned} y_{k,m,n}^r(t;\Theta) &= \xi\phi_m(t - \tau(t;\Theta)) e^{j2\pi f_{p_m}(t-\tau(t;\Theta))} e^{j\varphi_k} \\ &\approx \xi\phi_m(t - kT_{PRI} - \tau(r)) e^{j2\pi f_{p_m}(t-\tau(r))} \\ &\quad \times e^{-j2\pi f_{p_m}\tau(\theta)} e^{-j2\pi f_{p_m}\tau(vt)} e^{j\varphi_k} \end{aligned} \tag{5}$$

where ξ is the target reflection coefficient. $\tau_{k,m,n}(t;\Theta) = \tau(r) + \tau(\theta) + \tau(vt)$ is the two-way time delay of the transmit signals. $\tau(r) = 2r/c$, $\tau(\theta) = -md\sin\theta/c - nd\sin\theta/c$, and $\tau(vt) = -2vkT_{PRI}/c$,, v denotes the radial velocity, c is the speed of light. The approximation in (5) is due to the fact that $\phi_m(t - \tau_{k,m,n}) \approx \phi_m(t - \tau(r))$ holds under the narrow-band assumption. For simplicity, we define $e_m(t) = e^{j2\pi f_{p_m}t}$ and $\omega_m(t) = e^{-j2\pi f_{p_m}\tau(vt)} = e^{j2\pi\eta_m f_d t}$, where $\eta_m = f_{p_m}/f_c, f_d = 2vf_c/c$. So we have $\mathbf{e}(t) = [e_0(t), e_1(t), \ldots, e_{M-1}(t)]^T$ and $\mathbf{\Omega}(t) = diag\{\omega_0(t), \omega_1(t), \ldots, \omega_{M-1}(t)\}$. Then, the

received signal can be written in the following vector form

$$\mathbf{y}^r(t) = \xi \mathbf{a}_r(\theta)\mathbf{a}_t^T(\theta)\mathbf{e}(t-\tau(r)) \times \sum_{k=0}^{K-1}\mathbf{\Omega}(t)\phi_m(t-kT_{PRI}-\tau(r)) \quad (6)$$

where $\mathbf{a}_t(\theta) = \left[1, e^{j2\pi d\sin\theta/\lambda}, \cdots, e^{j2\pi(M-1)d\sin\theta/\lambda}\right]^T$ and $\mathbf{a}_r(\theta) = \left[1, e^{j2\pi d\sin\theta/\lambda}, \cdots, e^{j2\pi(N-1)d\sin\theta/\lambda}\right]^T$ are the steering vectors of the transmit and receive arrays, respectively. It's noticed that the phase term $e^{j\varphi_k}$ is a constant for each radar pulse which can be absorbed into ξ. Suppose the radar pulse duration satisfies $Tf_d \ll 1$, the intra-pulse Doppler frequency shift can be ignored, then, we can have

$$\begin{aligned}&\sum_{k=0}^{K-1}\mathbf{\Omega}(t)\phi_m(t-kT_{PRI}-\tau)\\ &\approx \sum_{k=0}^{K-1}\mathbf{\Omega}(kT_{PRI}+\tau;f_d)\phi_m(t-kT_{PRI}-\tau)\\ &\approx e^{j2\pi f_d\tau}\sum_{k=0}^{K-1}\mathbf{\Omega}(kT_{PRI};f_d)\phi_m(t-kT_{PRI}-\tau)\end{aligned} \quad (7)$$

Denote $\tau(r) = \tau$ and $\mathbf{\Omega}(kT_{PRI};f_d) = \mathbf{\Omega}_k(f_d)$, the receive signal of the radar pulse in the kth PRI is given by

$$\mathbf{y}_k^r(t) = \xi \mathbf{a}_r(\theta)\mathbf{a}_t^T(\theta)\mathbf{\Omega}_k(f_d)\boldsymbol{\phi}_k(t-\tau)\mathbf{e}(t-\tau) \quad (8)$$

where $\boldsymbol{\phi}_k(t) = diag\{\phi_0(t-kT_{PRI}),\ldots,\phi_{M-1}(t-kT_{PRI})\}$ and $\mathbf{\Omega}_k(f_d) = diag\left\{e^{j2\pi\eta_0 f_d kT_{PRI}},\ldots,e^{j2\pi\eta_{M-1}f_d kT_{PRI}}\right\}$. After down converting and matched filtering of the received signal, the data matrix can be expressed as

$$\begin{aligned}\mathbf{y}_k^r &= \int_{-\infty}^{\infty}\mathbf{y}_k(t)\mathbf{e}^*(t)\boldsymbol{\phi}_k^*(t-\tau')dt\\ &= \xi\mathbf{a}_r(\theta)[\mathbf{\Omega}_k(f_d)\mathbf{a}_t(r,\theta)]^T\mathbf{R}_\phi(t-\Delta\tau)\end{aligned} \quad (9)$$

where $\mathbf{a}_t(r,\theta) = \mathbf{a}_t(\theta)\odot\mathbf{e}^*(\tau)$ is range-angle-dependent transmit steering vector, $\mathbf{R}_\phi(t-\Delta\tau) = \int_T \phi_m(t)\phi_n^*(t-\Delta\tau)dt$ is the covariance matrix of the transmit signals. Since the transmit signals of FDA-MIMO radar are orthogonal, $\mathbf{R}_\phi(t-\Delta\tau) = \mathbf{I}_M$, $\mathbf{I}_M$ is $M\times M$ identity matrix. The discrete receive signal model in the kth radar pulse are finally written as

$$\mathbf{y}_k^r = \xi\mathbf{a}_r(\theta)[\mathbf{\Omega}_k(f_d)\mathbf{a}_t(r,\theta)]^T \quad (10)$$

In order to obtain the discrete received signal model in the dimensions of transmit spatial, receive spatial and temporal, we can vectorize $\mathbf{y}_k^r \in \mathbb{C}^{N\times M}$ by column and it yields $vec(\mathbf{y}_k) = \xi\mathbf{\Omega}_k(f_d)\mathbf{a}_t(r,\theta)\otimes\mathbf{a}_r(\theta)$. Then, we denote

$$\left[vec^T(\mathbf{y}_0), vec^T(\mathbf{y}_1),\ldots,vec^T(\mathbf{y}_{K-1})\right]^T = \xi\mathbf{h}(r,\theta,f_d) \quad (11)$$

in which the three-dimensional discrete data model of the K radar pulses is given by

$$\mathbf{h}(r,\theta,f_d) = \begin{bmatrix}(\mathbf{\Omega}_0(f_d)\mathbf{a}_t(r,\theta))\otimes\mathbf{a}_r(\theta)\\ \vdots\\ (\mathbf{\Omega}_{K-1}(f_d)\mathbf{a}_t(r,\theta))\otimes\mathbf{a}_r(\theta)\end{bmatrix} \quad (12)$$

where $\mathbf{h}\in\mathbb{C}^{KNM\times 1}$, it can be seen as the the joint range-space-time (RST) steering vector of the pulsed random FDA-MIMO radar.

C. COMMUNICATION SUBSYSTEM

The hybrid information embedding strategy of the proposed system include both index modulation and phase modulation, wherein the index modulation is realized by the selection and permutation of the transmit signals of classic FDA-MIMO radar. At the transmitter, M baseband waveforms are selected from the available orthogonal waveform set $\mathcal{S}$ with cardinality L, and there are $Q = C_L^M$ subsets in total, that is, the waveform dictionary can be denoted as $\mathbb{D} = \{\mathcal{S}_1,\mathcal{S}_2,\ldots,\mathcal{S}_Q\}$, $\mathcal{S}_q\subset\mathcal{S}, q = 1,\ldots,Q$. The selected M orthogonal waveform in $\mathcal{S}_q$ are then shuffled and assigned to the antenna array. Since the purpose of communication demodulating and decoding is quite different from radar subsystem, we can first rewrite the transmit signal model in the following vector form

$$\mathbf{x}_{k,\ell}^c(t) = \Phi_k\mathbf{P}_{k,\ell}\mathbf{S}(t)\mathbf{a}_t(\theta) \quad (13)$$

where $\Phi_k = e^{j\varphi_k}$ is the phase modulation term of the kth pulse. $\mathbf{P}_{k,\ell}\in\{0,1\}^{M\times M}, \ell = 1,\ldots,M!$ is the permutation matrix. The selected M transmit signals are listed in the diagonal matrix $\mathbf{S}(t) = diag\{\phi_0(t)e^{j2\pi f_0 t},\phi_1(t)e^{j2\pi f_1 t},\ldots,\phi_{M-1}(t)e^{j2\pi f_{M-1}t}\}$ and $f_m = f_c + m\Delta f$. $\mathbf{a}_t(\theta)$ denotes the phase difference caused by element spacing.

Under the far-field narrow band assumption, the channel response can be modeled as the frequency non-selective fading channel, the sub-channel is i.i.d and obeys Rayleigh fading. Suppose the channel matrix $\mathbf{H}_k\in\mathbb{C}^{N\times M}$ can be accurately estimated, thus, it is considered to be known in this paper. After channel transmission, the received signal on the nth antenna element can be expressed as

$$y_{k,n}^c(t) = \mathbf{h}_{k,n}^T\Phi_k\mathbf{P}_{k,\ell}\mathbf{S}(t)\mathbf{a}_t(\theta) + z_{k,n}^c(t) \quad (14)$$

where $\mathbf{h}_{k,n} = \left[h_{k,n,0}, h_{k,n,1},\ldots,h_{k,n,M-1}\right]^T$ is the mth row vector of $\mathbf{H}_k$, $h_{k,n,m}$ is the channel coefficient between the mth transmit antenna and the nth receive antenna of the kth pulse. Therefore, $\mathbf{h}_{k,n}$ denotes the channel coefficient from M transmit antennas to the nth receive element, it remains unchanged during the entire processing interval. $z_{k,n}^c(t)$ summarizes the unwanted clutter, interference and noise. Applying matched filtering and discretization of the received

signal, we can get

$$\begin{aligned}\mathbf{y}_{k,n}^{c} &= \int_{T} y_{k,n}^{c}(t)\, vec\left(\mathbf{S}^{*}(t)\right) dt \\ &= \int_{T} \left[\mathbf{h}_{k,n}^{T}\Phi_{k}\mathbf{P}_{k,\ell}\mathbf{S}(t)\,\mathbf{a}_{t}(\theta) + z_{k,n}^{c}(t)\right] vec\left(\mathbf{S}^{*}(t)\right) dt \\ &= \Phi_{k}\mathbf{h}_{k,n} \odot \mathbf{P}_{k,\ell}\mathbf{a}_{t}(\theta) + \mathbf{z}_{k,n}^{c} \end{aligned} \tag{15}$$

where $\mathbf{y}_{k,n}^{c}, \mathbf{z}_{k,n}^{c} \in \mathbb{C}^{M\times 1}$ are respectively the demodulated symbols vector and noise vector on the nth antenna element. With the threshold detection of $\mathbf{y}_{n}^{c}$, the selected waveform set $\mathcal{S}_{q}$ can be recovered.

The data symbols from N receive antennas can then be stacked into $\mathbf{y}_{k}^{c} = [\mathbf{y}_{k,0}^{c}, \mathbf{y}_{k,1}^{c}, \ldots, \mathbf{y}_{k,N-1}^{c}]^{T} \in \mathbb{C}^{N\times M}$. For the multi-channel receiver of the joint system, the maximum ratio combining (MRC) technique, which can fully utilize the receiving diversity, are applied to maximize the SNR of the received signals. For MRC, the weight vector $\mathbf{w}_{k} = \mathbf{h}_{k,m}^{*}$, $\mathbf{h}_{k,m}$ is the nth column vector of $\mathbf{H}_{k}$. That is to say, the weight factors in each antenna should be matched to the corresponding channel. Let $\mathbf{w}_{k} = [w_{k,0}, w_{k,1}, \ldots, w_{k,N-1}]^{T}$, $\mathbf{y}_{k,m}^{c} = [y_{k,0,m}, y_{k,1,m}, \ldots, y_{k,N-1,m}]^{T}$ denotes the mth column of $\mathbf{y}_{k}^{c}$, so the mth received symbols can be combined by the weighted sum $Y_{k,m} = \mathbf{w}_{k}^{T}\mathbf{y}_{k,m}^{c} = \sum_{n=0}^{N-1} w_{k,n}y_{k,n,m}$. In such case, the received data symbol vector can be written as

$$\mathbf{Y}_{k}^{c} = \Phi_{k}\mathbf{P}_{k,\ell}\mathbf{a}_{t}(\theta) + \mathbf{Z}_{k}^{c} \tag{16}$$

where $\mathbf{Y}_{k}^{c} = \left[Y_{k,0}, Y_{k,1}, \ldots, Y_{k,M-1}\right]^{T}$ and $\mathbf{Z}_{k}^{c} = \left[Z_{k,0}, Z_{k,1}, \ldots, Z_{k,M-1}\right]^{T}$, and $Z_{k,m} = \sum_{n=0}^{N-1} w_{k,n}z_{k,n,m}$. Then, the permutation matrix $\mathbf{P}_{k,\ell}$ can be estimated by the following maximum likelihood (ML) detector

$$\hat{\mathbf{P}}_{k,\ell} = \arg\min_{\mathbf{P}} \left\|\mathbf{Y}_{k}^{c} - \Phi_{k}\mathbf{P}_{k,\ell}\mathbf{a}_{t}(\theta)\right\|_{2}^{2} \tag{17}$$

Finally, the phase term of the kth pulse can be calculated by $\varphi_{k} = \angle Y_{k,m} - 2\pi p_{k,m}d\sin\theta/\lambda$, and $\angle(\cdot)$ stands for the phase calculation operation. The main computational burden of the whole process lies in the ML estimation, we enumerate all the permutations to obtain the optimal permutation by exhaustive searching, and set M to a rather small value.

III. RANGE, ANGLE AND DOPPLER RESOLUTION

The Woodward's ambiguity function is commonly employed to characterize the radar resolution of different target parameters in range and Doppler, thus, the definition of ambiguity function can be extended to the cross-correlation function of two waveforms with different parameters. For the RFDA-MIMO radar subsystem of the proposed joint system, the generalized parameterized waveform can be expressed as

$$\mathbf{r}_{k}(t;\Theta) = \mathbf{a}_{r}(\theta)\,\mathbf{a}_{t}^{T}(\theta)\,\mathbf{\Omega}(t)\,\boldsymbol{\phi}_{k}(t-\tau)\,\mathbf{e}(t-\tau) \tag{18}$$

where $\Theta = (r, \theta, v)$ denotes the interested target parameters. The generalized ambiguity function (GAF), which is defined in [40] for MIMO radar, reveals a fact that the ambiguity function of MIMO radar is composed of the transmit and receive array steering vectors, as well as an inner product term related to the auto-correlation function of signals. Herein, we can represent the GAF for FDA-MIMO radar as

$$\begin{aligned}&\chi(\Theta_{1},\Theta_{2}) \\ &= \left|\int_{-\infty}^{\infty} \mathbf{r}_{k}(t;\Theta_{1})\,\mathbf{r}_{k}^{*}(t;\Theta_{2})\,dt\right| \\ &= \left|\int_{-\infty}^{\infty} \mathbf{e}^{H}(t-\tau_{2})\phi_{k}^{H}(t-\tau_{2})\,\mathbf{\Omega}^{H}(t)\,\mathbf{a}_{t}^{*}(\theta_{2})\,\mathbf{a}_{r}^{H}(\theta_{2})\right. \\ &\quad \left.\times\mathbf{a}_{r}(\theta_{1})\,\mathbf{a}_{t}^{T}(\theta_{1})\,\mathbf{\Omega}(t)\,\phi_{k}(t-\tau_{1})\,\mathbf{e}(t-\tau_{1})\,dt\right| \\ &\approx \left|\mathbf{a}_{t}^{H}(r_{2},\theta_{2})\,\mathbf{R}_{k}(\Delta\tau,\Delta f)\,\mathbf{a}_{r}^{H}(\theta_{2})\,\mathbf{a}_{r}^{H}(\theta_{2})\,\mathbf{a}_{t}^{H}(r_{1},\theta_{1})\right| \end{aligned} \tag{19}$$

The approximation in the formula results from $\mathbf{\Omega}(t) \approx \omega_{0}(t)\,\mathbf{I}_{M}$, which means the Doppler shift in each pulse keeps constant when the transmit signals are assumed to be narrowband. Under the narrow band assumption, the inner product matrix $\mathbf{R}_{k}(\Delta\tau,\Delta f)$, which is also called the narrow-band covariance function, can be given by

$$\begin{aligned}&\mathbf{R}_{k}(\Delta\tau,\Delta f) \\ &= \int_{-\infty}^{\infty} \phi_{k}^{H}(t-\tau_{2})\,\mathbf{e}^{H}(-\tau_{2})\,\phi_{k}(t-\tau_{1})\,\mathbf{e}(-\tau_{1})\,dt \\ &= \int_{-\infty}^{\infty} \phi_{k}^{H}(t-\tau_{2})\,\phi_{k}(t-\tau_{1})\,e^{-j2\pi\eta_{1}f_{d}t}e^{j2\pi\eta_{2}f_{d}t}dt \\ &= \int_{-\infty}^{\infty} \phi_{k}^{H}(t)\,\phi_{k}(t-\Delta\tau)\,e^{-j2\pi\Delta f_{d}t}dt \end{aligned} \tag{20}$$

where $\Delta\tau = \tau_{1} - \tau_{2}$ and $\Delta f_{d} = (\eta_{1} - \eta_{2})f_{d}$. It's noted that the conventional ambiguity function of FDA-MIMO radar is similar to the ambiguity function of MIMO radar, which is determined by the covariance matrix of transmit signals and the transmit and receive array steering vectors.

However, due to the utilization of multi-frequency transmission, FDA-based array radar can experience severe Doppler ambiguity. The Doppler dimension profile of the ambiguity function of FDA-MIMO radar has periodic spikes in $n\Delta f, n \in \mathbb{Z}$, if the mainlobe is located in $n = 0$, the others can result in severe Doppler ambiguity. It's not appropriate to adopt fast-time Doppler estimation by matched filtering of the radar signals to measure the Doppler frequency shift of moving targets [41]. Besides, the transmit baseband signal of which can employ pulse train signals. The pulse width of the single waveform is rather small, and the frequency offset satisfies $\Delta f \ll f_{c}$. Thus, under the narrow band assumption, the Doppler spread caused by frequency offset in the slow time scale can be ignored in signal modeling of pulsed FDA-based array radar in current studies.

To avoid the Doppler ambiguity and further investigate the impact of Doppler spread on radar resolution, the Doppler measurements should be conducted in slow time domain. Firstly, we introduce the range-space-time (RST) response of pulsed RFDA-MIMO radar signal based on the three-dimensional discrete data model $\mathbf{h}(r,\theta,f_{d})$ to analyze the

radar resolution in slow time domain. First, we define

$$\mathcal{H}(\Delta r, \Delta \sin\theta, \Delta f_d) = \frac{1}{KMN}\mathbf{h}^H(r,\theta,f_d)\mathbf{h}(r',\theta',f_d') \tag{21}$$

where $\Delta r = r' - r$, $\Delta \sin\theta = \sin\theta' - \sin\theta$ and $\Delta f_d = f_d' - f_d$. As well, the RST response is composed of Doppler spread $\mathbf{\Omega}_k(f_d)$, the transmit and receive array steering vectors. It can be regarded as a slow-time ambiguity function of pulsed FDA-MIMO radar, and be employed to characterize radar resolution performance in range, angle and Doppler domains. Substitute the 3D signal model $\mathbf{h}$ in (12) into (20), we can obtain the RST response as follows

$$\begin{aligned}
&\mathcal{H}(\Delta r, \Delta \sin\theta, \Delta f_d) \\
&= \frac{1}{KMN}[\Omega_k(f_d)\,\mathbf{a}_t(r,\theta) \otimes \mathbf{a}_r(\theta)]^H \\
&\quad \times [\Omega_k(f_d)\,\mathbf{a}_t(r,\theta) \otimes \mathbf{a}_r(\theta)] \\
&= \frac{1}{KMN}\sum_{n=0}^{N-1}\sum_{m=0}^{M-1}\sum_{k=0}^{K-1} e^{-j2\pi p_m \Delta f \Delta\tau} e^{j2\pi\eta_m \Delta f_d k T_{PRI}} \\
&\quad \times e^{j2\pi nd\Delta\sin\theta/\lambda} e^{j2\pi md\Delta\sin\theta/\lambda}
\end{aligned} \tag{22}$$

In fact, if we don't consider the influence of Doppler spreading effect on radar resolution performance, the RST model can be seen as a simplification of the generalized ambiguity function. In subsequent, the range, angle and Doppler profile of the RST response can be calculated by

$$\mathcal{H}(0, \Delta\sin\theta, 0) = \frac{1}{MN}\left|\sum_{m=0}^{M-1}\sum_{n=0}^{N-1} e^{j\frac{2\pi nd\Delta\sin\theta}{\lambda}} e^{j\frac{2\pi md\Delta\sin\theta}{\lambda}}\right| \tag{23a}$$

$$\mathcal{H}(\Delta r, 0, 0) = \frac{1}{M}\left|\sum_{m=0}^{M-1} e^{-j4\pi p_m \Delta f \Delta r/c}\right| \tag{23b}$$

$$\mathcal{H}(0, 0, \Delta f_d) = \frac{1}{KM}\left|\sum_{m=0}^{M-1}\sum_{k=0}^{K-1} e^{j2\pi\eta_m \Delta f_d k T_{PRI}}\right| \tag{23c}$$

From (23), we can notice that the introduction of randomness in carrier frequency for FDA-MIMO radar have no influence on the angle resolution. The radar subsystem of the proposed joint system should have the same angle resolution as conventional MIMO radar and FDA radar.

IV. MAINLOBE INTERFERENCE SUPPRESSION

At present, most researches on the design of radar and communication dual-function system based on a multi-antenna system mainly focus on the conventional PA and MIMO radar. Due to the angle-dependent array factor, both PA and MIMO radar can only deal with the sidelobe interferences, while the mainlobe jamming can not be suppressed effectively due to lack of extra DOFs. When the deceptive jamming appears in the radar mainlobe region and have the same direction angle with the true target, they can not be distinguished. Compared to PA and MIMO radar, the transmit beampattern of FDA-MIMO radar are range-angle dependent, in such case, the true target and the deceptive target with an identical angle can be distinguishable in range domain.

Since the radar Doppler processing usually happens in slow time domain, which is independent of the processing in range and angle dimension, the Doppler term is omitted hereafter for the sake of simplicity. When the time domains are neglected, we can denote the simplified discrete signal model as follows

$$\mathbf{y}^r = \eta\mathbf{a}_t(r,\theta) \otimes \mathbf{a}_r(\theta) + \mathbf{z}^r \tag{24}$$

where $\eta = \xi e^{j\varphi_k} e^{-j2\pi f_c \tau(r)}$. Under narrow-band assumption, the transmit steering vector can be expressed as

$$\begin{aligned}
\mathbf{a}_t(r,\theta) = \Big[1, e^{-j2\pi p_1 \Delta f \tau(r)} e^{j2\pi d\sin\theta/\lambda}, \ldots, \\
e^{-j2\pi p_{M-1}\Delta f\tau(r)} e^{j2\pi(M-1)d\sin\theta/\lambda}\Big]^T
\end{aligned} \tag{25}$$

Suppose that a target is located at (r_0, θ_0) and the interferer is located at (r_i, θ_i), the received signal model of the RFDA-MIMO radar subsystem is given by

$$\mathbf{y}^r = \eta_0\mathbf{a}_t(r_0,\theta_0) \otimes \mathbf{a}_r(\theta_0) + \eta_i\mathbf{a}_t(r_i,\theta_i) \otimes \mathbf{a}_r(\theta_i) + \mathbf{z}^r \tag{26}$$

where η_0 and η_j are respectively the constant coefficient of the target and the interferer.

If the target and interferer are not in the same angle, i.e. $\theta_0 \neq \theta_i$, a blocking matrix processing method proposed in [32] can be used to deal with jammer suppression. By designing a blocking matrix based on the receive steering vector, the jamming signals can be totally cancelled. The blocking matrix is

$$\mathbf{B} = \begin{bmatrix} 1 & -e^{j2\pi d\sin\theta_i/\lambda} & \cdots & 0 \\ 0 & 1 & \cdots & 0 \\ \vdots & \vdots & \ddots & \vdots \\ 0 & 0 & 1 & -e^{j2\pi d\sin\theta_i/\lambda} \end{bmatrix}. \tag{27}$$

The jamming signals can be suppressed by $\mathbf{y}_b^r = \mathbf{B}\mathbf{y}^r$. Then, the traditional beamforming algorithm, such as minimum variance distortionless response (MVDR) and subspace algorithm, can be applied to estimate the range and angle of desired target. However, we can notice that, if $\theta_0 = \theta_i$, the target signals may also be canceled.

The transmit-receive beampattern of FDA-MIMO radar is range-dependent, which can be exploited to distinguish the targets with the same direction but different distances. Hence, in this section, we adopt an eigenvalue projection-based algorithm for RFDA-MIMO radar subsystem to suppress mainlobe jamming signals. Ignoring η_0 and η_i, the jamming signal model can be written as $\mathbf{y}_i = \mathbf{a}_t(r_i,\theta_i) \otimes \mathbf{a}_r(\theta_i)$. Based on the blocking matrix processing principle [42], the projection matrix is given by

$$\bar{\mathbf{A}} = \mathbf{I} - \frac{\mathbf{a}_t(r_i,\theta_i)\,\mathbf{a}_t^H(r_i,\theta_i)}{\mathbf{a}_t^H(r_i,\theta_i)\,\mathbf{a}_t(r_i,\theta_i)} \tag{28}$$

where $\mathbf{I}$ is an $M \times M$ identity matrix. Define $\mathbf{A} = \left[\bar{\mathbf{A}}\ \bar{\mathbf{A}} \cdots \bar{\mathbf{A}}\right]$, $\mathbf{A} \in \mathbb{C}^{M \times MN}$, and then, we can have

$$\mathbf{A}\mathbf{y}_i = \left[\bar{\mathbf{A}} \quad \bar{\mathbf{A}} \quad \cdots \quad \bar{\mathbf{A}}\right]\left[\mathbf{a}_t(r_i, \theta_i) \otimes \mathbf{a}_r(\theta_i)\right] = \mathbf{0} \quad (29)$$

where $\mathbf{0}$ is an $M \times 1$ zero vector. That is to say, the jamming signal is successfully suppressed. When the target and interferer are in the mainlobe of RFDA-MIMO radar beampattern and have the different ranges, the target signal can be preserved in the suppression process.

Denote $\mathbf{u}(r, \theta) = \mathbf{a}_t(r, \theta) \otimes \mathbf{a}_r(\theta)$, the interference plus noise covariance matrix is given by

$$\mathbf{R}_{i+z} = \sigma_i^2 \mathbf{u}(r_i, \theta_i)\, \mathbf{u}^H(r_i, \theta_i) + \mathbf{R}_z \quad (30)$$

where $\sigma_i^2 = E\left\{\eta_i^2\right\}$ denote the variance of the interference. The output SINR can be calculated as

$$\begin{aligned} \mathrm{SINR} &= \frac{E\left\{|\eta_0 \mathbf{A}\mathbf{u}(r_0, \theta_0)|^2\right\}}{E\left\{|\eta_i \mathbf{A}\mathbf{u}(r_i, \theta_i) + \mathbf{A}\mathbf{z}^r|^2\right\}} = \frac{\sigma_i^2 |\mathbf{A}\mathbf{u}(r_0, \theta_0)|^2}{\mathbf{A}\mathbf{R}_{i+z}\mathbf{A}^H} \\ &= \sigma_i^2 \mathbf{u}^H(r_0, \theta_0)\, \mathbf{R}_{i+z}^{-1} \mathbf{u}(r_0, \theta_0) \end{aligned} \quad (31)$$

V. COMMUNICATION SECURITY ENHANCEMENT

Due to the higher spatial freedom, multi-antenna technology can effectively improve physical layer security of wireless communication. For phase array radar, the directional modulation technique is an effective way to achieve secure information transmission. The modulation process happens in the RF module of the transmitter rather than the baseband signal, making the transmitted signal to be direction-dependent. The directional beam of phase array radar can radiate the beampattern in the direction of the desired receiver while suppressing the beampattern in other directions. However, if the eavesdropper and the target user are at different distances in the same direction, it obviously can not guarantee the communication security in range dimension.

The range-angle dependent beampattern of the FDA-MIMO radar provides the possibility of solving this problem. In this section, we propose an approach to enhance the communication security of the proposed joint system, which aims to maximize the signal power in the desired direction of the target user and minimize it in the direction of the eavesdropper, reducing the possibility of communication being eavesdropped in both range and angle dimension. With the far-field assumption, and neglect the amplitude attenuation and noise in free space transmission, the received signal points, that is, the output of the mth matched filter on the nth receive antenna of the kth pulse can be expressed as

$$\begin{aligned} y_{k,m,n}(r, \theta) &= w_m e^{-j2\pi(f_c + p_m \Delta f)\tau(r)} e^{-j2\pi(f_c + p_m \Delta f)\tau(\theta)} e^{j\varphi_k} \\ &= w_m e^{-j2\pi f_c \tau(r)} e^{-j2\pi p_m \Delta f \tau(r)} e^{j2\pi m d \sin\theta/\lambda} \\ &\quad \cdot e^{j2\pi n d \sin\theta/\lambda} e^{j\varphi_k}. \end{aligned} \quad (32)$$

This is a general signal model for both radar and communication subsystem. w_m is the undetermined weight on the mth transmit antenna. Add up all the received symbols obtained from each channel, it yields

$$\begin{aligned} E_k(r, \theta, \mathbf{w}) &= \sum_{n=0}^{N-1} \sum_{m=0}^{M-1} y_{k,m,n}(r, \theta) \\ &= e^{j\varphi_k} e^{-j2\pi f_c \tau(r)} \sum_{n=0}^{N-1} e^{j2\pi n d \sin\theta/\lambda} \\ &\quad \cdot \sum_{m=0}^{M-1} w_m e^{-j2\pi p_m \Delta f \tau(r)} e^{j2\pi m d \sin\theta/\lambda} \\ &= \alpha_k \sum_{n=0}^{N-1} \sum_{m=0}^{M-1} w_m a_{r,n}(\theta)\, a_{t,m}(\theta)\, e_m^*(\tau) \end{aligned}$$

where the constant term $\alpha_k = e^{j\varphi_k} e^{-j2\pi f_c \tau(r)}$. However, if the receive steering vector $\mathbf{a}_r(\theta)$ is considered, the FDA-MIMO array radar can generate $M \times N$ virtual beam just like MIMO radar, which results in the false targets in the angle profile at the receiver. Owing to the multiple-channel receiver structure, the communication symbols can be received and demodulated in each antenna. Thus, in order to guarantee the transmit beam can arrive at the desired target, we can denote the received signal points on the nth antenna as

$$E_{k,n}(r, \theta, \mathbf{w}) = \alpha_k \mathbf{w}^T \mathbf{a}_t(r, \theta). \quad (33)$$

where the complex weighted vector $\mathbf{w} = [w_0, w_1, \ldots, w_{M-1}]^T$. By choosing an appropriate $\mathbf{w}$, the signal power of the synthesized signal at the target user's position can be manipulated. Suppose the target users set and the eavesdropper set are respectively given by $U = \left\{u_1, u_2, \ldots, u_{|U|}\right\}^T$, $V = \left\{v_1, v_2, \ldots, v_{|V|}\right\}^T$, where $|U|$ and $|V|$ denote the number of elements in set U and set V, the optimization function can then be expressed as

$$\begin{aligned} \max_{\mathbf{w}} F_k = &\sum_{i=1}^{|U|} \omega(u_i) \left\|E_{u,k}(r_{ui}, \theta_{ui}, \mathbf{w})\right\|^2 \\ &- \sum_{j=1}^{|V|} \omega(v_j) \left\|E_{v,k}(r_{vj}, \theta_{vj}, \mathbf{w})\right\|^2 \end{aligned} \quad (34)$$

where $\omega(u_i)$ and $\omega(v_j)$ are the weights for the ith target user and the jth eavesdropping user, respectively. $E_{u,k}(r_{ui}, \theta_{ui}, \mathbf{w}), i = 1, 2, \ldots, |U|$ and $E_{v,k}(r_{vj}, \theta_{vj}, \mathbf{w}), j = 1, 2, \ldots, |V|$ are the received signal points at the position of target users and eavesdroppers. Due to the range-angle-dependent transmit-receive beampattern of FDA-MIMO radar, the solution of optimization problem $\mathbf{w}$ is related to the targets' range and angle, which can be utilized to control the received signal power of the targets and eavesdroppers with the same angle but different ranges. However, it is difficult for the optimization problem to obtain an explicit expression. Specially, if we only consider one target user u_1 without reckoning on the eavesdroppers, the optimization function can be expressed as

$$\max_{\mathbf{w}} F_k = \left\|\alpha_k \mathbf{w}^T \mathbf{a}_t(r_{u1}, \theta_{u1})\right\|^2 \quad (35)$$

Then, we can get the explicit expression of the complex weighted vector

$$\mathbf{w} = \alpha_k \mathbf{a}_t^* (r_{u1}, \theta_{u1}) \tag{36}$$

in which $w_m = \alpha_k^* e^{j2\pi p_m \Delta f \tau(r_{u1})} e^{-j2\pi md \sin\theta_{u1}/\lambda}$. In such case, the received signal power can be maximized in the position of the target user u_1.

For the proposed RFDA-MIMO joint system scheme, the index modulation scheme embeds the information bits through the shuffling of the transmit FDA-MIMO waveform. At the receiver of communication subsystem, the matched filter output can be seen as a permutation of the transmit steering vector. In other words, it utilizes the phase shifts of the antenna elements to carry messages, which implies its angle dependency. By introducing a weighted vector, the information transmission will be range-angle dependent, avoiding the communication security loss between eavesdroppers and target users at different distances in the same direction. Thereby, the communication security performance can be enhanced.

VI. UPPER BOUND OF SYMBOL ERROR RATE

Without loss of generality, the transmitted symbols $\mathbf{x}_{k,\ell}$ are considered to be the discretization of matched filter output of the transmit signal $\mathbf{x}_{k,\ell}^c(t)$, which is $\mathbf{x}_{k,\ell} = \Phi_k \mathbf{P}_{k,\ell} \mathbf{a}_t(\theta)$. The received symbols are denoted by $\mathbf{y}_k$. Define the distance between the received symbols $\mathbf{y}_k$ and the ith code $\mathbf{x}_{k,i}$, $\forall i, i = 1, \ldots, M!, i \neq \ell$ as $D_{k,i} = \left\|\mathbf{y}_k - \mathbf{x}_{k,i}\right\|_2$. In the kth pulse, thereby, the probability of a correct symbol detection can be expressed as

$$\begin{aligned} P(no\ error\ |\varphi_k) &= P\left(D_{k,\ell} < D_{k,i}\right) \\ &\geq \prod_{m=0}^{M-1} P\left(D_{k,m,\ell} < D_{k,m,i}\right) \end{aligned} \tag{37}$$

where $P\left(D_{k,m,\ell} < D_{k,m,i}\right)$ denotes the probability of a correct detection of the mth phase term. The phase rotation for the mth antenna is $\psi_m = \varphi_{k,m} + 2\pi p_m d \sin\theta/\lambda$, and the phase difference is $\Delta\psi_{k,m} = \Delta\varphi_{k,m} + 2\pi md \sin\theta/\lambda$, $m = 0, 1, \ldots, M-1$, where $\Delta\varphi_{k,m} = 2\pi/J$. Hence, we can have the largest phase spread can be given by

$$\psi_{\max} = \frac{2\pi(J-1)}{J} + \frac{2\pi(M-1)d\sin\theta_c}{\lambda} = 2\pi \tag{38}$$

To avoid the angular ambiguity, it is advantageous to transmitted at the maximal spread angle $\theta_c = \sin^{-1}\left(\frac{\lambda}{(M-1)dJ}\right)$. On the single antenna, the distance between two different signal points is $d_{\min} = \sqrt{2E_s}\sin\Delta\psi_{k,m}$. The symbol error rate (SER) on the mth antenna can be calculated as the SER of the traditional M-ary phase shift keying (MPSK) modulation, which can be approximated by

$$P_{e,m} \approx 2Q\left(\frac{d_{\min}}{\sqrt{N_0}}\right) \approx 2Q\left(\sqrt{2\gamma_s}\sin\Delta\psi_m\right) \tag{39}$$

where $\gamma_s = E_s/N_0$ denotes the symbol SNR, N_0 is the noise power spectral density. $Q(x) = \frac{1}{2}erfc\left(x/\sqrt{2}\right)$, and $erfc(x)$ is the standard complementary error function. Then, we can have

$$P\left(D_{k,m,\ell} < D_{k,m,i}\right) = 1 - 2Q\left(\sqrt{2\gamma_s}\sin\Delta\psi_{k,m}\right)$$

where $\Delta\psi_m = \min\left\{\Delta\psi_{k,m}\right\}$. Since $P(error\ |\varphi_k) = 1 - P(no\ error\ |\varphi_k)$, the upper bound of the correct symbol detection probability under the condition of φ_k is represented as

$$P(error\ |\varphi_k) \leq 1 - \left[1 - P_{e,m}\right]^M \tag{40}$$

Now, the average SER of the whole joint system can be calculated as

$$P_s = \sum_{j=0}^{J-1} P(error\ |\varphi_k)\, P(\varphi_k) \tag{41}$$

In fact, the embedded phase term φ_k occurs in equal probability and keeps the same for all the receive antennas in each pulse. Hence, we have $P(\varphi_k) = 1/J$. The upper bound of the SER is finally given by

$$P_s \leq 1 - \left[1 - 2Q\left(\sqrt{2\gamma_s}\sin\Delta\psi_m\right)\right]^M \tag{42}$$

TABLE 1. Simulation parameters.

Parameter	Value	Parameter	Value
Carrier frequency f_c	10 GHz	Element spacing d	0.015 m
Frequency offset Δf	10 kHz	Number of element M, N	8
Pulse duration T	10 μs	Number of waveform L	12
Signal bandwidth	30MHz	Target position	$(10km, 10^\circ)$
Number of pulses K	100	SNR	10dB
PRF f_{PRF}	10kHz	SIR	5dB

VII. SIMULATION RESULTS

In this section, we keep forward to discuss the potential of the proposed scheme as a joint radar and communication system, including the performance of radar resolution and the system anti-interference capability, and the communication security approach which take advantage of the range-angle dependent feature of the FDA-MIMO radar. For brevity, we first make a list of the simulation parameters in Table 1.

A. RADAR RESOLUTION

Based on the range, angle and Doppler profiles of the RST response, the radar resolution performance of the proposed joint system can be predicted. Fig.4 compares the range resolution of the proposed RFDA-MIMO radar and conventional linear FDA-MIMO radar. The GAF of linear FDA-MIMO radar can be deduced in [41] when the transmit signals are orthogonal. The horizontal axis represents the normalized range difference $\Delta r/r_{bin}$, $r_{bin} = c/2B$ is the size of range bin. When $\Delta f = B$, the range resolution of the RFDA-MIMO radar is better than that of the linear FDA-MIMO radar. Moreover, as the frequency increment Δf gets larger, the range resolution can be improved to some extent. However, when $\Delta f \geq 2B$, the grating lobes appears in a range

unit, which results in range ambiguities within a range cell. The comparison of angle resolution is shown in Fig.5, the proposed radar subsystem have the same angle resolution as the conventional FDA-MIMO radar, which is consistent with the theoretical expression.

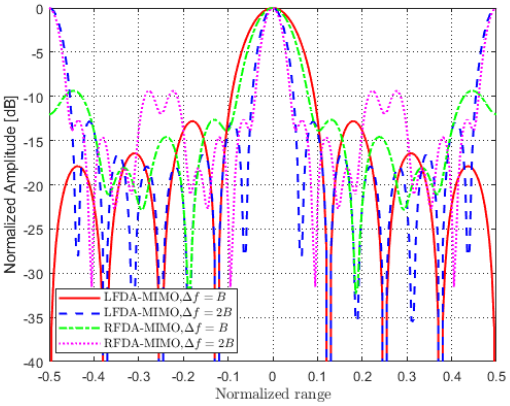

FIGURE 4. Range profile of the RST response.

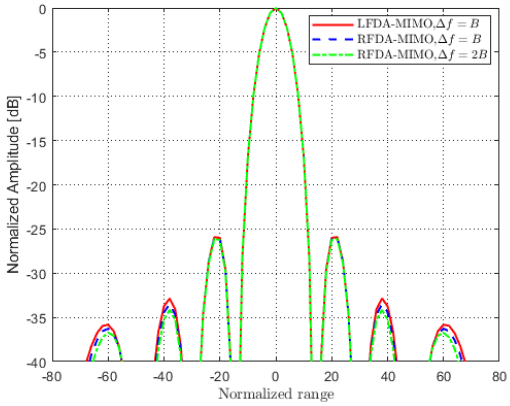

FIGURE 5. Angle profile of the RST response.

Fig.6 presents the Doppler profile of the RST response, with the horizontal axis being the normalized Doppler difference. Just as the normal radar, the pulsed FDA-MIMO radar subsystem utilize staggered PRI to resolve Doppler ambiguity. According to the expression (22c), the Doppler resolution can be approximated as $\Delta f_d \approx 1/\eta_{M-1}KT_{PRI}$. Since $1/\eta_{M-1} \approx 1$, the Doppler resolution of RFDA-MIMO radar basically identical with the conventional PA radar, MIMO radar or FDA radar. The Doppler ambiguity can generate period peak in k/T_{PRI} in the Doppler profile, as illustrated in Fig.6. Increasing the number of snapshots K, the Doppler resolution of RFDA-MIMO radar can be improved, the amplitude of the grating lobe are about to decrease. While if Δf becomes larger, the Doppler resolution only slightly improve.

In this simulation, we can see that the randomization in carrier frequency of FDA-MIMO radar have no influence on the radar angle resolution, it has the same angle resolution as some other conventional array radar systems. Besides, due to the modulus operation, the range and Doppler resolution of RFDA-MIMO radar only have a small improvement compared with the linear FDA-MIMO radar.

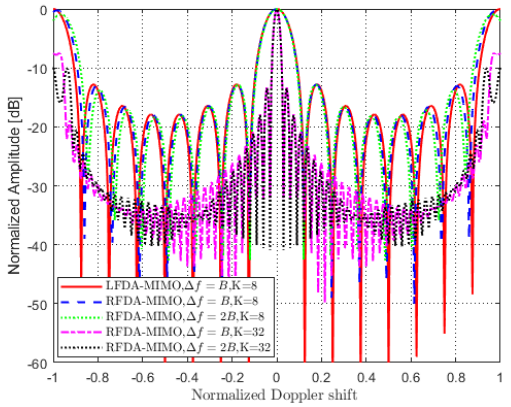

FIGURE 6. Doppler profile of the RST response.

B. ANTI-INTERFERENCE PERFORMANCE ANALYSIS

Attribute to the range-angle dependent transmit-receive beampattern of the FDA-MIMO radar, joint mainlobe interference suppression from both range and angle dimensions can be in progress via beamforming approach. Fig.7 compares the interference suppression results between RFDA-MIMO radar and MIMO radar. Compared Fig.7(a) and Fig.7(b), we can see that MIMO radar cannot discriminate two targets locating in the same angle but distinct ranges, while the RFDA-MIMO radar can successfully suppress the interference and localized the target with the same angle through MVDR beamforming. Suppose the target is located at $T_0 = (10km, 10°)$, Fig.7(b) and Fig.7(c) shows the interference suppression results when the jammer are respectively located at $T_i = (15km, 10°)$ and $T_i = (10km, 15°)$, which demonstrates its advantage in joint range and angle interference suppression. However, as shown in Fig.7(c), mainlobe distortion can appear at the target position when using MVDR beamforming. The eigenvalue projection algorithm provides a solution for this problem, of which the results are shown in Fig.7(d). Nevertheless, it should be noted that the priori information of the real target are needed for this method.

In order to evaluate the suppression performance, the output SINR versus SNR for various situations are shown in Fig.8. Simulations using Monte Carlo experiments with 200 trials are carried out. For comparison, the output SINR of the received signals without jammer suppression is plotted in red solid line. the signal-to-noise ratio (SNR) and the signal-to-interference ratio (SIR) are set to $SNR = 10dB$ and $SIR = 5dB$, respectively. Under MVDR beamforming, the output SINR has been greatly improved for both of the two radar arrays, the proposed RFDA-MIMO radar can have

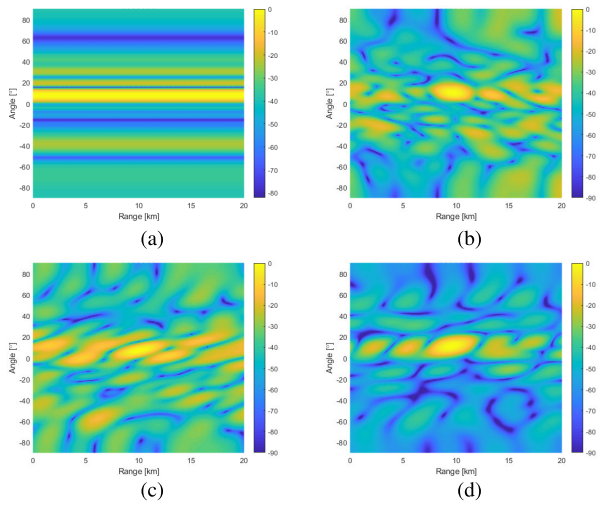

FIGURE 7. Interference suppression results for target and jammer. (a) MIMO radar using MVDR, $T_0 = (10km, 10°)$, $T_j = (15km, 10°)$. (b) RFDA-MIMO radar using MVDR, $T_0 = (10km, 10°)$, $T_j = (15km, 10°)$. (c) RFDA-MIMO radar using MVDR, $T_0 = (10km, 10°)$, $T_j = (10km, 15°)$. (d) RFDA-MIMO radar using the eigenvalue projection-based approach, $T_0 = (10km, 10°)$, $T_j = (10km, 15°)$.

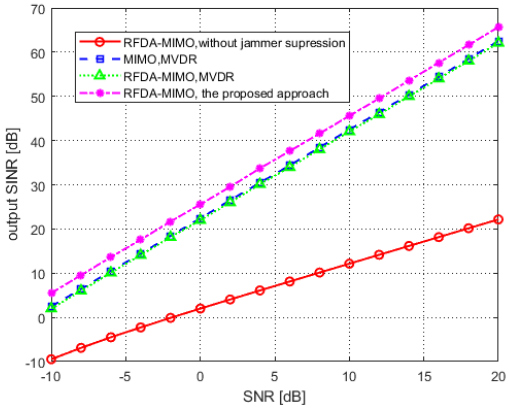

FIGURE 8. Comparisons of the output SINR.

almost the same output SINR as the MIMO radar. However, the proposed interference suppression approach can achieve a higher SINR level than the systems using the MVDR beamforming method.

C. COMMUNICATION SUBSYSTEM EVALUATION

We continue to examine the communication performance of the proposed joint system scheme in this subsection. Fig.9 depicted the SER performance of various radar systems in range-angle two-dimensional (2D) plane. In the simulation, the target user is located at $(10km, 10°)$, two eavesdroppers are located at $(15km, 10°)$ and $(10km, 30°)$. The weighted vector $\mathbf{w}$ is obtained by finding the minimum value of the function using genetic algorithm. Then, the SER can be calculated in light of the signal points received at each position of the current receiver. Fig.9(a) is obtained based on the directional modulation using PA in [38], which utilize the phase shifts and weighting to carry information bits. Obviously, the SER of the directional modulation is only a function of angle, which means if the eavesdroppers are in the same direction but different ranges, the target users can also have the possibility of being eavesdropped. For the conventional linear FDA-MIMO radar, the weighted vector is determined by only considering the transmit steering vector. The SER results are shown in Fig.9(b), the communication performance can be better in the S-shaped dark blue positions. Different from the PA radar, the SER of LFDA-MIMO radar is range-angle related, which can realize the secure transmission in specific ranges and directions.

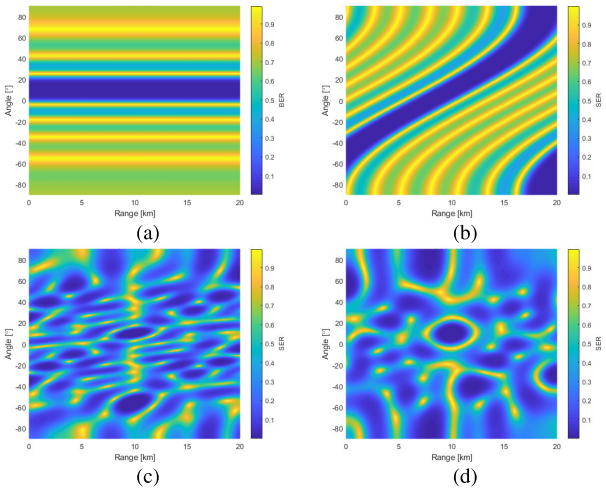

FIGURE 9. The SER performance in range-angle 2D plane. (a) PA. (b) LFDA-MIMO. (c) RFDA-MIMO (virtual). (d) RFDA-MIMO.

Fig.9(c) illustrates the SER results of the RFDA-MIMO radar if considering both the transmit and receive steering vectors. Due to the synthesized the virtual beampattern, a false low SER region appears in the range-angle plane. That is to say, the information bits can also be received and demodulated if the eavesdroppers lies in this area. For the proposed multiple-channel receiver, the communication information can be obtained in each antenna element. Hence, we only consider using the transmit steering vector to determine the weighted values. The corresponding SER results are shown in Fig.9(d). We can see that the SER is rather low at the target user location $(10km, 10°)$, while the SER at the position of eavesdropping users $(15km, 10°)$ and $(10km, 30°)$ is close to 0.9, which is completely unable to demodulate communication information.

In order to intuitively evaluate the safety of the proposed communication subsystem, the SER performance in range profile and angle profile are provided in Fig.10. Fig.10(a) compares the SER results of range dimension profiles of various systems. The SER of PA radar kept at constant value 3×10^{-4}, which means it can not ensure secure communication in range dimension. At the position of the

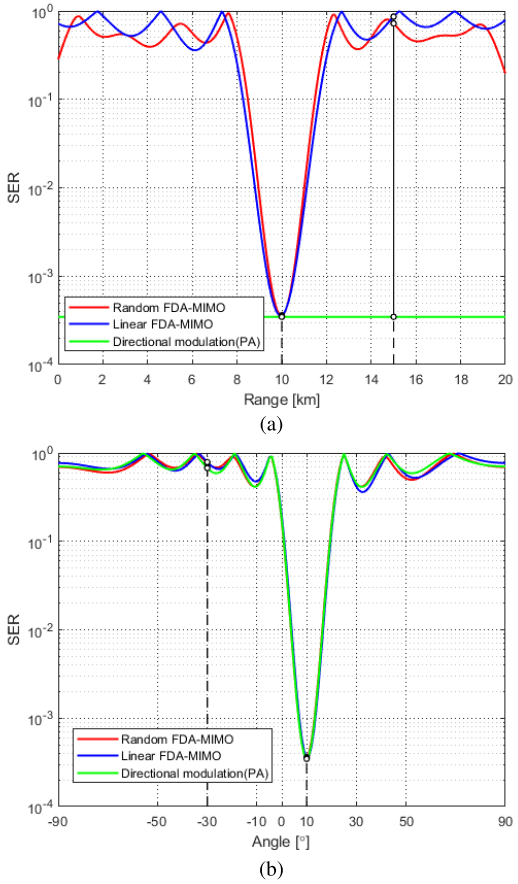

FIGURE 10. The SER performance in different dimensions. (a) SER in range dimension. (b) SER in angle dimension.

target user, both of the LFDA-MIMO and RFDA-MIMO system have a valley, but the mainlobe width of RFDA-MIMO is smaller than that of the conventional LFDA-MIMO system. While at the position of eavesdropping users, the SER level of both the two system scheme can be very high. The SER results in angle dimension profile are presented in Fig.10(b), the mentioned three systems have similar safety performance in the target user location, and the SER level of the directional modulation using PA is lower than both the LFDA-MIMO and RFDA-MIMO system schemes.

Fig.11 depicts the SER verses SNR for various the modulation order J and the transmit antenna number M. To avoid angular ambiguity, the communication direction is set to $\theta_c = \sin^{-1}\left(\frac{\lambda}{(M-1)dJ}\right)$. Clearly, the slope of SER versus SNR curve goes to infinity as SNR becomes large. As expected, the SER performance exhibit worse when J and M are increasing, for the reason that the distance between the signal points are getting closer. In particular, we observed the crossover of SER curves when $M = 8, J = 8$ and $M = 2, J = 16$, which means the SER performance can be anomalous when adopting different combination plans of M and J. Hence, it is crucial to customize a suitable modulation

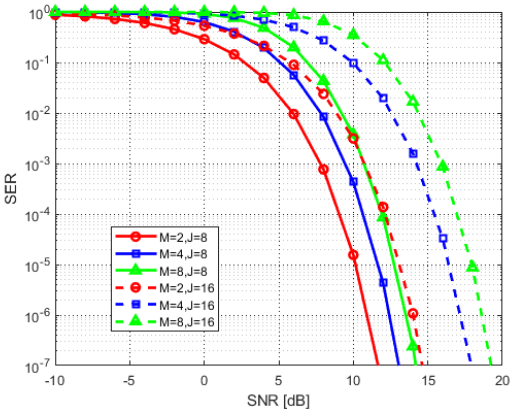

FIGURE 11. Comparative SER performance among different M and J.

scheme for the joint systems to trade off the data rate and the communication reliability.

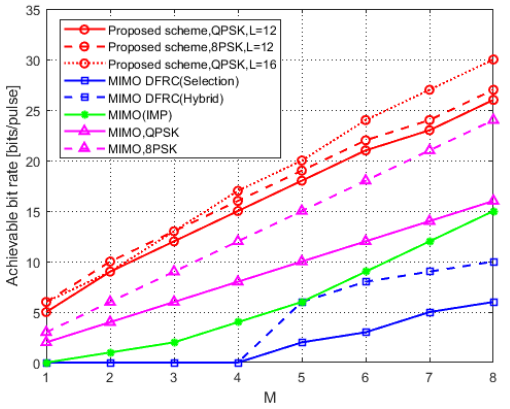

FIGURE 12. Comparative achievable bit rate among different systems.

Finally, we compare the achievable data rate versus the transmit antenna number M of various communication system schemes. In this experiment, the number of selected antenna in MIMO DFRC system is set to $K = 4$. The MIMO DFRC system, proposed in [25], adopt two different schemes: the antenna-selection-based index modulation strategy with the bit rate $\left\lfloor \log_2\left(\binom{M}{K}\right)\right\rfloor$ and the hybrid antenna selection and permutation strategy with the bit rate $\left\lfloor \log_2\left(\binom{M}{K}\right) + \log_2 K!\right\rfloor$. Observing Fig.12, we can see that the bit rate of MIMO DFRC systems are the lowest due to restriction of the active antenna numbers. The following one is the data rate of MIMO radar that only utilize index modulation via permutation (IMP) for information embedding [21], which is $\lfloor \log_2 M! \rfloor$. Furthermore, the proposed system scheme outperforms that of traditional MIMO communication with QPSK and 8PSK modulation schemes, for sake of simultaneously utilizing phase modulation and index modulation approach.

VIII. CONCLUSION

In this paper, we investigated the performance of the proposed joint radar and communication system based on FDA-MIMO radar, and demonstrated its functionality and superiority compared with some existed dual-function system schemes based on conventional PA and MIMO radar. The range-angle-Doppler 3D signal model is derived for the radar subsystem to analyze the radar resolution in range, angle and Doppler dimensions. Due to the randomization in frequency offsets of the transmit signals, the radar resolution can be improved. The angle and Doppler resolution are not affected compared with the linear FDA-MIMO radar. Owing to the angle-range dependent beampattern, the RFDA-MIMO radar subsystem can suppress the interference with the same direction but different distances. Furthermore, we proposed an approach to enhance communication safety by maximizing the signal power in the desired direction of the target user, making it more safe to convey information bits in different ranges and angles. Besides, the upper bound of the SER is theoretically deduced and analyzed, which is conducive to determine the modulation mode to make balance between the communication data rate and reliability. Simulation results indicate that compared with other joint systems based on PA and MIMO radar, the proposed joint radar and communication system scheme has a great potential in future applications.

REFERENCES

[1] F. Liu, C. Masouros, A. Li, H. Sun, and L. Hanzo, "MU-MIMO communications with MIMO radar: From co-existence to joint transmission," *IEEE Trans. Wireless Commun.*, vol. 17, no. 4, pp. 2755–2770, Apr. 2018.

[2] B. Li, A. P. Petropulu, and W. Trappe, "Optimum co-design for spectrum sharing between matrix completion based MIMO radars and a MIMO communication system," *IEEE Trans. Signal Process.*, vol. 64, no. 17, pp. 4562–4575, Sep. 2016.

[3] X. Liu, T. Huang, N. Shlezinger, Y. Liu, J. Zhou, and Y. C. Eldar, "Joint transmit beamforming for multiuser MIMO communications and MIMO radar," *IEEE Trans. Signal Process.*, vol. 68, pp. 3929–3944, 2020.

[4] J. Qian, M. Lops, L. Zheng, X. Wang, and Z. He, "Joint system design for coexistence of MIMO radar and MIMO communication," *IEEE Trans. Signal Process.*, vol. 66, no. 13, pp. 3504–3519, Jul. 2018.

[5] M. Rihan and L. Huang, "Optimum co-design of spectrum sharing between MIMO radar and MIMO communication systems: An interference alignment approach," *IEEE Trans. Veh. Technol.*, vol. 67, no. 12, pp. 11667–11680, Dec. 2018.

[6] P. Ren, A. Munari, and M. Petrova, "Performance tradeoffs of joint radar-communication networks," *IEEE Wireless Commun. Lett.*, vol. 8, no. 1, pp. 165–168, Feb. 2019.

[7] F. Wang, A. L. Swindlehurst, and H. Li, "Joint antenna selection and transmit beamforming for dual-function radar-communication systems," in *Proc. IEEE Radar Conf.*, May 2023, pp. 1–6.

[8] C. Sturm and W. Wiesbeck, "Waveform design and signal processing aspects for fusion of wireless communications and radar sensing," *Proc. IEEE*, vol. 99, no. 7, pp. 1236–1259, Jul. 2011.

[9] F. Liu, L. Zhou, C. Masouros, A. Li, W. Luo, and A. Petropulu, "Toward dual-functional radar-communication systems: Optimal waveform design," *IEEE Trans. Signal Process.*, vol. 66, no. 16, pp. 4264–4279, Aug. 2018.

[10] S. Shi, Z. Wang, Z. He, and Z. Cheng, "Constrained waveform design for dual-functional MIMO radar-communication system," *Signal Process.*, vol. 171, Jun. 2020, Art. no. 107530.

[11] W. Wu, G. Han, Y. Cao, Y. Huang, and T.-S. Yeo, "MIMO waveform design for dual functions of radar and communication with space-time coding," *IEEE J. Sel. Areas Commun.*, vol. 40, no. 6, pp. 1906–1917, Jun. 2022.

[12] X. Chen, X. Wang, S. Xu, and J. Zhang, "A novel radar waveform compatible with communication," in *Proc. Int. Conf. Comput. Problem-Solving (ICCP)*, Oct. 2011, pp. 177–181.

[13] J. Jakabosky, S. D. Blunt, and B. Himed, "Waveform design and receive processing for nonrecurrent nonlinear FMCW radar," in *Proc. IEEE Radar Conf.*, May 2015, pp. 1376–1381.

[14] A. Hassanien, M. G. Amin, Y. D. Zhang, and F. Ahmad, "A dual function radar-communications system using sidelobe control and waveform diversity," in *Proc. IEEE Radar Conf.*, May 2015, pp. 1260–1263.

[15] A. Hassanien, M. G. Amin, Y. D. Zhang, and F. Ahmad, "Phase-modulation based dual-function radar-communications," *IET Radar, Sonar Navigat.*, vol. 10, no. 8, pp. 1411–1421, Oct. 2016.

[16] T. Huang, N. Shlezinger, X. Xu, Y. Liu, and Y. C. Eldar, "MAJoRCom: A dual-function radar communication system using index modulation," *IEEE Trans. Signal Process.*, vol. 68, pp. 3423–3438, 2020.

[17] W. Baxter, E. Aboutanios, and A. Hassanien, "Joint radar and communications for frequency-hopped MIMO systems," *IEEE Trans. Signal Process.*, vol. 70, pp. 729–742, 2022.

[18] J. Jian, W.-Q. Wang, B. Huang, L. Zhang, M. A. Imran, and Q. Huang, "MIMO-FDA communications with frequency offsets index modulation," *IEEE Trans. Wireless Commun.*, early access, pp. 1–17, 2023.

[19] E. Basar, M. Wen, R. Mesleh, M. Di Renzo, Y. Xiao, and H. Haas, "Index modulation techniques for next-generation wireless networks," *IEEE Access*, vol. 5, pp. 16693–16746, 2017.

[20] N. Ishikawa, S. Sugiura, and L. Hanzo, "50 years of permutation, spatial and index modulation: From classic RF to visible light communications and data storage," *IEEE Commun. Surveys Tuts.*, vol. 20, no. 3, pp. 1905–1938, 3rd Quart., 2018.

[21] E. BouDaher, A. Hassanien, E. Aboutanios, and M. G. Amin, "Towards a dual-function MIMO radar-communication system," in *Proc. IEEE Radar Conf.*, May 2016, pp. 1–6.

[22] W. Baxter, H. Nosrati, and E. Aboutanios, "A study on the performance of symbol dictionary selection for the frequency hopped DFRC scheme," in *Proc. IEEE Radar Conf.*, Sep. 2020, pp. 1–6.

[23] D. Ma, N. Shlezinger, T. Huang, Y. Shavit, M. Namer, Y. Liu, and Y. C. Eldar, "Spatial modulation for joint radar-communications systems: Design, analysis, and hardware prototype," *IEEE Trans. Veh. Technol.*, vol. 70, no. 3, pp. 2283–2298, Mar. 2021.

[24] D. Ma, N. Shlezinger, T. Huang, Y. Liu, and Y. C. Eldar, "FRaC: FMCW-based joint radar-communications system via index modulation," *IEEE J. Sel. Topics Signal Process.*, vol. 15, no. 6, pp. 1348–1364, Nov. 2021.

[25] X. Wang, A. Hassanien, and M. G. Amin, "Dual-function MIMO radar communications system design via sparse array optimization," *IEEE Trans. Aerosp. Electron. Syst.*, vol. 55, no. 3, pp. 1213–1226, Jun. 2019.

[26] T. Huang, N. Shlezinger, X. Xu, D. Ma, Y. Liu, and Y. C. Eldar, "Multi-carrier agile phased array radar," *IEEE Trans. Signal Process.*, vol. 68, pp. 5706–5721, 2020.

[27] W.-Q. Wang, "Frequency diverse array antenna: New opportunities," *IEEE Antennas Propag. Mag.*, vol. 57, no. 2, pp. 145–152, Apr. 2015.

[28] K. Gao, W. Wang, J. Cai, and J. Xiong, "Decoupled frequency diverse array range–angle-dependent beampattern synthesis using non-linearly increasing frequency offsets," *IET Microw., Antennas Propag.*, vol. 10, no. 8, pp. 880–884, Jun. 2016.

[29] Y. Liu, H. Ruan, L. Wang, and A. Nehorai, "The random frequency diverse array: A new antenna structure for uncoupled direction-range indication in active sensing," *IEEE J. Sel. Topics Signal Process.*, vol. 11, no. 2, pp. 295–308, Mar. 2017.

[30] W.-Q. Wang, H. C. So, and A. Farina, "An overview on time/frequency modulated array processing," *IEEE J. Sel. Topics Signal Process.*, vol. 11, no. 2, pp. 228–246, Mar. 2017.

[31] R. Gui, W.-Q. Wang, C. Cui, and H. C. So, "Coherent pulsed-FDA radar receiver design with time-variance consideration: SINR and CRB analysis," *IEEE Trans. Signal Process.*, vol. 66, no. 1, pp. 200–214, Jan. 2018.

[32] W.-Q. Wang, H. C. So, and A. Farina, "FDA-MIMO signal processing for mainlobe jammer suppression," in *Proc. 27th Eur. Signal Process. Conf. (EUSIPCO)*, Sep. 2019, pp. 1–5.

[33] L. Lan, J. Xu, G. Liao, Y. Zhang, F. Fioranelli, and H. C. So, "Suppression of mainbeam deceptive jammer with FDA-MIMO radar," *IEEE Trans. Veh. Technol.*, vol. 69, no. 10, pp. 11584–11598, Oct. 2020.

[34] S. Y. Nusenu and W.-Q. Wang, "Dual-function FDA MIMO radar-communications system employing Costas signal waveforms," in *Proc. IEEE Radar Conf.*, Apr. 2018, pp. 0033–0038.

[35] S. Ji, W.-Q. Wang, H. Chen, and S. Zhang, "On physical-layer security of FDA communications over Rayleigh fading channels," *IEEE Trans. Cognit. Commun. Netw.*, vol. 5, no. 3, pp. 476–490, Sep. 2019.

[36] A. Basit, S. Yaw Nusenu, W. Khan, S. Khan, S. Wali, M. Arshad, and A. Waseem, "Adaptive main lobe/sidelobes controls selection in FDA based joint radar-communication design," in *Proc. Int. Conf. Electr., Commun., Comput. Eng. (ICECCE)*, Jul. 2019, pp. 1–5.

[37] M. Li and W.-Q. Wang, "Joint radar-communication system design based on FDA-MIMO via frequency index modulation," *IEEE Access*, vol. 11, pp. 67722–67736, 2023.

[38] M. P. Daly and J. T. Bernhard, "Directional modulation technique for phased arrays," *IEEE Trans. Antennas Propag.*, vol. 57, no. 9, pp. 2633–2640, Sep. 2009.

[39] M. P. Daly, E. L. Daly, and J. T. Bernhard, "Demonstration of directional modulation using a phased array," *IEEE Trans. Antennas Propag.*, vol. 58, no. 5, pp. 1545–1550, May 2010.

[40] G. San Antonio, D. R. Fuhrmann, and F. C. Robey, "MIMO radar ambiguity functions," *IEEE J. Sel. Topics Signal Process.*, vol. 1, no. 1, pp. 167–177, Jun. 2007.

[41] R. Gui, B. Huang, W.-Q. Wang, and Y. Sun, "Generalized ambiguity function for FDA radar joint range, angle and Doppler resolution evaluation," *IEEE Geosci. Remote Sens. Lett.*, vol. 19, pp. 1–5, 2022.

[42] O. Hoshuyama, A. Sugiyama, and A. Hirano, "A robust adaptive beamformer for microphone arrays with a blocking matrix using constrained adaptive filters," *IEEE Trans. Signal Process.*, vol. 47, no. 10, pp. 2677–2684, Jul. 1999.

MENGJIAO LI received the B.S. degree from the North China University of Water Resources and Electric Power, and the M.S. degree from the University of Electronic Science and Technology of China, Chengdu, in 2018, where she is currently pursuing the Ph.D. degree. Her research interests include joint radar and communication waveform design and frequency diverse array signal processing.

WEN-QIN WANG (Senior Member, IEEE) received the B.E. degree in electrical engineering from Shandong University, Shandong, China, in 2002, and the M.E. and Ph.D. degrees in information and communication engineering from the University of Electronic Science and Technology of China (UESTC), Chengdu, China, in 2005 and 2010, respectively. From March 2005 to 2007, he was with the National Key Laboratory of Microwave Imaging Technology, Chinese Academy of Sciences, Beijing, China. Since September 2007, he has been with the School of Information and Communication Engineering, UESTC, where he is currently a Professor and the Director. From June 2011 to May 2012, he was a Visiting Scholar with the Stevens Institute of Technology, Hoboken, NJ, USA. From December 2012 to December 2013, he was a Hong Kong Scholar with the City University of Hong Kong, Hong Kong. From January 2014 to January 2016, he was a Marie Curie Fellow with the Imperial College London, U.K. His research interests include the area of array signal processing and circuit systems for radar, communications, and microwave remote sensing.